

# Monte Carlo simulation of carbon ion radiotherapy for the human eye

PANG Cheng-Guo(庞成果)<sup>1,2;1)</sup> SU You-Wu(苏有武)<sup>2</sup> WANG Wen-Jun(王文军)<sup>3</sup> LUO Xiao-Ming(罗晓明)<sup>4</sup>  
 XU Jun-Kui(徐俊奎)<sup>1,2</sup> LI Wu-Yuan(李武元)<sup>2</sup> YUAN Jiao(袁娇)<sup>2</sup> YAO Ze-En(姚泽恩)<sup>1</sup>

<sup>1</sup> School of Nuclear Science and Technology, Lanzhou University, Lanzhou 730000, China

<sup>2</sup> Institute of Modern Physics, Chinese Academy of Sciences, Lanzhou 730000, China

<sup>3</sup> Gansu National Health Inspection, Lanzhou 730000, China

<sup>4</sup> The People's Hospital of Linze, Zhangye 734000, China

**Abstract:** Carbon ion is the mostly common used particle in heavy ion radiotherapy. In this paper, the carbon ion dose in tumor treatment for human eye was calculated with FLUKA code. An 80 MeV/u carbon beam was irradiated into the human eye from two directions. The first was from the lateral-forward direction, which was a typical therapeutic condition. In this case, a maximum dose was deposited in the tumor volume. In the second a beam was irradiated into eyes from the forward direction to simulate a patient gazing directly into treatment beam during therapy, which may cause a certain medical accident. This method can be used for a treatment plan in heavy ion radiotherapy.

**Key words:** carbon ion beam, FLUKA, dose distribution, human eye

**PACS:** 87.10.Rt, 29.27.-a **DOI:** 10.1088/1674-1137/39/1/018201

## 1 Introduction

Uveal melanoma is a common tumor in the eyes of adults and children, which accounts for about 12% of all melanomas [1]. Interiorly, its morbidity is just under the retinoblastoma. In terms of this kind of tumor, the usual therapies are ophthalmectomy, transpupillary thermotherapy, brachytherapy and etc. However, these methods have the same risk in that the tumor may be spread to another place or it may cause other serious consequences.

For uveal melanoma treatment, heavy ions therapy, especially using carbon ions, has many advantages. Firstly, carbon ions deposit their maximum energy density at the end of their track, which is the so called Bragg peak. A comparison for the Bragg peak of different particles is shown in Fig. 1 [2]. Secondly, carbon ions can easily be formed as narrow focused and scanning pencil beams of variable penetration depth, which are very important because the critical organs necessary for eyesight are located very close. Thirdly, compared with the proton beam, the carbon ion beam has a smaller lateral penumbra and a sharper dose distribution and, because of its character of high LET, the RBE value of carbon ion is higher than mostly common radiation. Lastly, the location where the dose is deposited by carbon ions can be determined by means of online positron emission tomography. With all the above features, carbon ion therapy

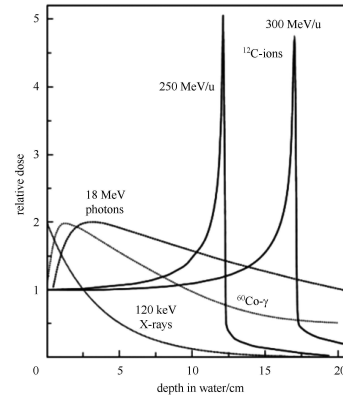


Fig. 1. A comparison of dose-depth distributions in the water of X-rays,  $^{60}\text{Co}$ - $\gamma$  rays, high energy photons and 250, 300 MeV/u carbon ions.

is expected to bring a very good therapeutic effect for large tumors located close to vital organs.

FLUKA is a general purpose tool that is used for calculations of particle transport and interactions with matter, which is jointly developed by the European Laboratory for Particle Physics (CERN) [3], and the Italian National Institute for Nuclear Physics (INFN) Sixty different particles plus heavy ions can be transported by this code over a wide energy range, so it is suitable for calculating the heavy ion dose in radiotherapy. The aim of this paper is to develop a simple model of the human eye to estimate the dose delivered from carbon ions

Received 5 March 2014

1) E-mail: pangchl3@lzu.edu.cn

©2015 Chinese Physical Society and the Institute of High Energy Physics of the Chinese Academy of Sciences and the Institute of Modern Physics of the Chinese Academy of Sciences and IOP Publishing Ltd

radiotherapy. The calculated dose includes that due to carbon ions and secondary particles.

## 2 Simulation of energy deposition in water

To simulate the dose distribution of the human eye, First of all, the range of 80, 85, 90, 95, and 100 MeV/u carbon ions in water was calculated with SRIM2013. The result is shown in Table 1.

Table 1. The range of different energy carbon irradiated into water.

energy/(MeV/u)	range/cm
80	1.73
85	1.94
90	2.14
95	2.36
100	2.59

Due to the small size of human eye, whose radius is about 1.3 cm, according to the range of carbon ions in tissue, an energy of 80 MeV/u for carbon ions is large enough for eye radiotherapy.

To verify whether the FLUKA code is suitable for heavy ions dose simulation in radiotherapy, the dose deposition of carbon ions with energy of 80 MeV/u in water was calculated beforehand. The calculated results are compared with the relative ionization energy-depth curve (Fig. 2) [4], and the good agreement indicates that FLUKA is effective for simulating heavy ions dose in radiotherapy.

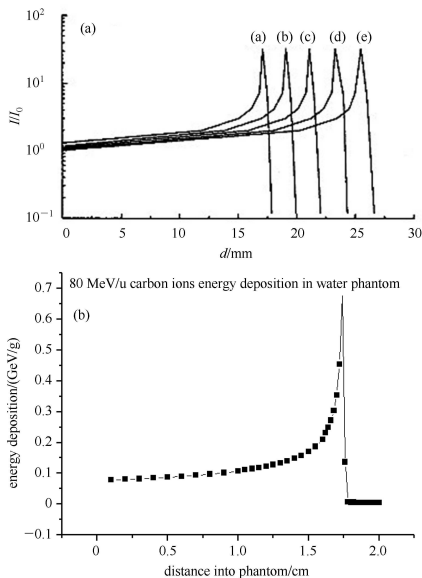


Fig. 2. Relative ionization energy-depth curve ((a), (a) 80 MeV/u, (b) 85 MeV/u, (c) 90 MeV /u, (d) 95 MeV/u, (e) 100 MeV/u), FLUKA simulation results (b).

## 3 FLUKA simulation

The two dimensional rendering of the eye used for the FLUKA modeling is shown in Fig. 3 [5]. Many uveal melanomas appear in the choroid and sclera structure of the eye. However, many critical structures of eye are radiosensitive, such as the lens, the cornea etc., and are located very close together. A cataract is one of the deterministic effects of radiation with relatively low threshold dose, which happens because radiation exposure to the cornea can cause the structure to become opaque and this leads to blindness. This should be considered carefully in the treatment and these critical areas should be distinguished in the model.

Overall, the model was constructed with a set of concentric spheres. The optic nerve is simulated as a cylinder appropriately offset at the posterior of the eye. Assuming that the cancerous tumor located in the volume  $R9$  in Fig. 3, the  $L1$  to  $L10$  and the  $R1$  to  $R10$  is ten dispersed volumes of left and right side of the eye model, respectively. We have simulated two cases in which the direction of the carbon beam is from a lateral forward ( $45^\circ$  to the line of centers of the set of concentric spheres) and a forward direction ( $18^\circ$  to the line of centers of the set of concentric spheres), respectively, as shown in Fig. 4.

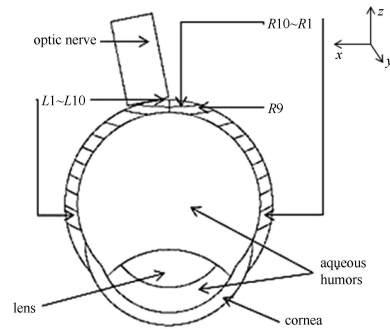


Fig. 3. FLUKA simulation model of human left eye.

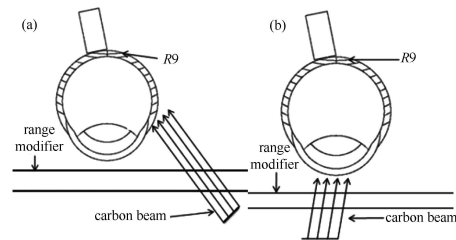


Fig. 4. Illustrations of lateral forward direction situation (a) and forward direction situation (b) geometry.

The material compositions of the eye were adapted from the ICRU Report 46 [6]. This report has addressed various tissues groups in the body and defined their elemental composition and density for purposes of radiation dosimetry. The lens of the eye is addressed directly in the MCNPX<sup>TM</sup> user's manual version 2.5.0 [7]. Recent

studies have indicated that the vitreous and the anterior humors have characteristics similar to the properties of lymph outlined in ICRU 46. Therefore, the composition of the vitreous and anterior is assumed to be the same as the lymph, the choroid and sclera are considered to be soft tissue, and the composition of the optic nerve was assumed to be the same as the rat's [8].

### 4 Results and analyses

The relative error ( $R$ ) of the simulation results is mainly caused by the statistical fluctuation, which can be controlled by changing the historical number of particles in the simulation. The relative errors for the two cases' treatment program were 0.0056 and 0.0038, respectively.

#### 4.1 The lateral forward direction situation

According to some recent studies, the lateral-forward direction therapeutic dose for uveal melanoma in the cancerous tumor volume  $R9$  is about 50 Gy, spread over four fractions, which translates into four treatments of 12.5 Gy delivered to the patient. The simulation results for the lateral-forward direction treatment program are found in Table 2. According to the results, the cancerous tumor volume  $R9$  gets the maximum dose (12.5019 Gy per fraction, 50.0078 Gy in total) while there is a minimizing dose elsewhere. The dose of the left side is at least three orders of magnitude lower than right side. The total dose to the optic nerve was only about 6.8764 Gy, This is within the acceptable limit of 10 Gy for the optic nerve during radiotherapy [9]. For each fraction the

cornea received less than 0.1 Gy, which is well within the acceptable limit of 15 Gy [10], For the lens of the eye, a special effort is made in radiotherapy to keep doses within an acceptable limit: usually less than 8 Gy. In this simulation, the cumulative dose to the lens of the eye from the four fractions was only 0.0024 Gy.

In this paper, we used a proper card USRBIN of FLUKA to score the dose distribution of each section for the eye model. Fig. 5 and Fig. 6 reveal the results of several sections: the dose is higher when the color is deeper.

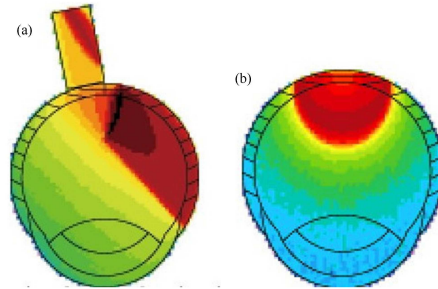


Fig. 5. (color online) Dose distribution for section when  $y=0$  cm (a), and  $x=0$  cm (b).

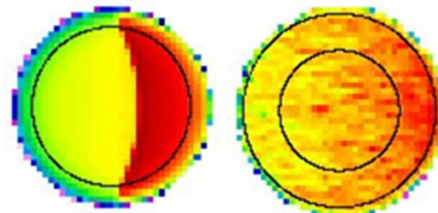


Fig. 6. (color online) Dose distribution for section at  $z=4.6$  cm (left), and  $z=2.3$  cm (right).

Table 2. Dose distribution for lateral-forward direction situation.

dose volume	dose per fraction/Gy	total dose/Gy
cornea	0.0134	0.0534
anterior humor	0.0005	0.0019
lens	0.0006	0.0024
vitreous humor	1.8266	7.3064
optic NERVE	1.7191	6.8764
$R1$	2.1192	8.4768
$R2$	2.2419	8.9679
$R3$	2.2137	8.8549
$R4$	2.1032	8.4128
$R5$	1.9426	7.7705
$R6$	2.0001	8.0005
$R7$	3.3672	13.4689
$R8$	10.5536	42.2142
$R9$	12.5019	50.0078
$R10$	7.5663	30.2654
$L1$	0.0003	0.0013
$L2$	0.0004	0.0017
$L3$	0.0007	0.0026
$L4$	0.0011	0.0039
$L5$	0.0017	0.0068
$L6$	0.0034	0.0136
$L7$	0.0108	0.0431
$L8$	0.0839	0.3358
$L9$	0.2041	0.8164
$L10$	0.2357	0.9427

Table 3. Dose distribution for forward direction situation.

dose volume	dose per fraction/Gy	total dose/Gy
cornea	1.3103	5.2411
anterior humor	4.1885	16.7538
lens	6.2868	25.1743
vitreous humor	1.9569	7.8276
optic NERVE	0.0028	0.0113
$R1$	0.0028	0.0113
$R2$	0.0039	0.0158
$R3$	0.0068	0.0273
$R4$	0.0156	0.0624
$R5$	0.0352	0.1409
$R6$	0.0551	0.2205
$R7$	0.0678	0.2713
$R8$	0.0747	0.2988
$R9$	0.0695	0.2781
$R10$	0.0568	0.2273
$L1$	0.0007	0.0029
$L2$	0.0006	0.0025
$L3$	0.0006	0.0025
$L4$	0.0007	0.0029
$L5$	0.0009	0.0037
$L6$	0.0013	0.0053
$L7$	0.0021	0.0085
$L8$	0.0049	0.019
$L9$	0.0127	0.0508
$L10$	0.0179	0.0719

## 4.2 The forward direction situation

For the forward direction scenario, we mimicked a patient gazing into the beam during treatment. The simulation results are shown in Table 3.

In accordance with Table 3, the majority of the energy is deposited in the lens, anterior humor, vitreous humor and cornea. However, the dose of the cancerous volume is almost zero. In this manner, just about 5.2411 Gy would be delivered to the cornea, which is well within the limits of 15 Gy. If this configuration occurred for the duration of the treatment, then the patient would suffer over 25 Gy to the lens. Compared to the accepted tolerable dose of 8 Gy, one would expect severe visual loss due to the lens becoming opaque during treatment. The dose distribution for the section of the eye model is illustrated in Fig. 7 and Fig. 8.

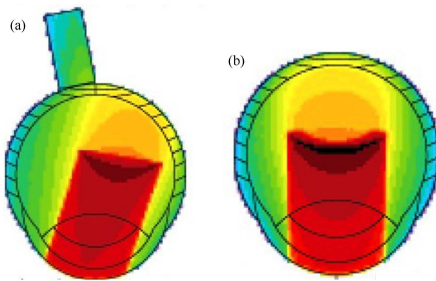


Fig. 7. (color online) Dose distribution for section when  $y=0$  cm (a), and  $x=0$  cm (b).

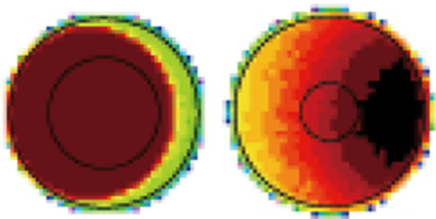


Fig. 8. (color online) Dose distribution for section at  $z=4.6$  cm (left), and  $z=2.3$  cm (right).

On this occasion, the carbon beam has not deposited its energy mainly in the tumor volume but in the lens, anterior humor, vitreous humor and cornea. This is caused

by the unexpected movement of the eyeball, which resulted in the depth of the tumor becoming longer than the lateral forward direction treatment program because of the change of direction while the energy of carbon beam was still 80 MeV/u during treatment.

## 5 Conclusion

The objective of this paper was to develop a model of the human eye using the computer code FLUKA that estimates of the dose delivered during radiotherapy. On the basis of the simulation results, we can draw the following conclusions:

1) The Monte Carlo simulation of heavy ions radiotherapy is a capable method that can be used to formulate the patient plan.

2) Results for the lateral forward direction treatment program indicate that it could be regarded as a typical treatment program because the dose to the tumor volume was at therapeutic levels and, at the same time, doses to the cornea, lens, and optic nerve were within acceptable limits.

3) For the forward direction situation, although the result was a large dose to the lens, the tumor received a very small dose because it is out of the range of carbon ion in this configuration. Compared with the result of the lateral forward direction situation, this scenario should be avoided in real radiotherapy. In the long term, this result could be used for dose distribution reconstruction in medical negligence cases.

There are also some problems that should be solved in future work. Greater details could be incorporated into the current of the eye, which would effectively expand the types of cancerous tumors that might be modeled. Regions outside the eye were neglected in the creation of this model. Inside the eye, greater accuracy could also be attained by adding more detail. Within the current eye model, it was not possible to simulate these types of tumors and their treatments. Likewise, greater resolution could be obtained by differentiating between organs that are located closely together in the eye.

## References

- 1 Harbour J W. Clinical Overview of Uveal Melanoma: Introduction to Tumors of the Eye. Ocular oncology. New York: Marcel Dekker, 2003, 1–18
- 2 YE Fei, LI Qiang. Nuclear Physics Review, 2010, **27**(3): 309 (in Chinese)
- 3 Ballarini F et al. Advances in Space Research, 2007, **40**(9): 1339
- 4 LI Qiang, WEI Zeng-Quan, DANG Bing-Rong et al. HEP & NP, 1997, **6**: 571–575 (in Chinese)
- 5 Atchison D A, Smith G, Smith G. Optics of the Human Eye. 2000. www.sciencedirect.com/science/book/978075063-7756
- 6 Photon E. Proton and Neutron Interaction Data for Body Tissues. ICRU Report, 1992, 46. <http://www.icru.org/home/reports/photon-electron-proton-and-neutron-interaction-data-for-body-tissues-report-46>
- 7 Pelowitz D B. MCNPX User's Manual Version 2.5. 0. Los Alamos National Laboratory, 2005. <http://library.lanl.gov/cgi-bin/getfile?00852475.pdf>
- 8 LoPachin R M, Stys P K. The Journal of Neuroscience, 1995, **15**(10): 6735–6746
- 9 Jones B, Errington R D. British Journal of Radiology, 2000, **73**(872): 802–805
- 10 šimonová G, Novotný J, Liščák R et al. Special Supplements, 2002, **97**: 635–639